

Title	Drastic reduction in the surface recombination velocity of crystalline silicon passivated with catalytic chemical vapor deposited SiN _x films by introducing phosphorous catalytic-doped layer
Author(s)	Trinh, Cham Thi; Koyama, Koichi; Ohdaira, Keisuke; Matsumura, Hideki
Citation	Journal of Applied Physics, 116(4): 044510-1-044510-7
Issue Date	2014-07-28
Type	Journal Article
Text version	publisher
URL	http://hdl.handle.net/10119/12905
Rights	Copyright 2014 American Institute of Physics. This article may be downloaded for personal use only. Any other use requires prior permission of the author and the American Institute of Physics. The following article appeared in Trinh Cham Thi, Koichi Koyama, Keisuke Ohdaira and Hideki Matsumura, Journal of Applied Physics, 116(4), 044510 (2014) and may be found at http://dx.doi.org/10.1063/1.4891237
Description	

Drastic reduction in the surface recombination velocity of crystalline silicon passivated with catalytic chemical vapor deposited SiN_x films by introducing phosphorous catalytic-doped layer

Trinh Cham Thi,^{1,2,a)} Koichi Koyama,^{1,2} Keisuke Ohdaira,^{1,2} and Hideki Matsumura^{1,2}

¹Japan Advanced Institute of Science and Technology (JAIST) 1-1 Asahidai, Nomi, Ishikawa 923-1292, Japan

²CREST, Japan Science and Technology Agency (JST) 4-1-8 Honcho, Kawaguchi, Saitama 332-0012, Japan

(Received 8 June 2014; accepted 13 July 2014; published online 28 July 2014)

We improve the passivation property of n-type crystalline silicon (c-Si) surface passivated with a catalytic chemical vapor deposited (Cat-CVD) Si nitride (SiN_x) film by inserting a phosphorous (P)-doped layer formed by exposing c-Si surface to P radicals generated by the catalytic cracking of PH₃ molecules (Cat-doping). An extremely low surface recombination velocity (SRV) of 2 cm/s can be achieved for 2.5 Ω cm n-type (100) floating-zone Si wafers passivated with SiN_x/P Cat-doped layers, both prepared in Cat-CVD systems. Compared with the case of only SiN_x passivated layers, SRV decreases from 5 cm/s to 2 cm/s. The decrease in SRV is the result of field effect created by activated P atoms (donors) in a shallow P Cat-doped layer. Annealing process plays an important role in improving the passivation quality of SiN_x films. The outstanding results obtained imply that SiN_x/P Cat-doped layers can be used as promising passivation layers in high-efficiency n-type c-Si solar cells. © 2014 AIP Publishing LLC. [<http://dx.doi.org/10.1063/1.4891237>]

I. INTRODUCTION

n-type crystalline silicon (c-Si) has recently become more and more attractive to photovoltaic research, raising forecast of switch from p-type to n-type c-Si solar cells on photovoltaic industry.^{1,2} Up to date, n-type c-Si solar cells are available, but their market share is at very low level (around 4%).² Nevertheless, the highest-efficiency solar cell has been recorded for an a-Si/n-type c-Si heterojunction back-contact solar cell in 2014.³ n-type c-Si solar cells have many advantages for realizing higher conversion efficiency than p-type wafer cells, such as no light-induced degradation and less effect of metal impurities, and their market share will thus increase in the near future, along with decrease in their process cost.^{1,4} Excellent passivation technique is of great importance particularly in improving back-contact c-Si solar cell efficiency. High-efficiency solar cells require surface passivation films not only with high transparency but also with high passivation ability so that photo-generated carriers do not recombine at the c-Si surface.⁵ Catalytic chemical vapor deposition (Cat-CVD),⁶ also referred to as hot-wire CVD, promises potential applications in passivation technique for c-Si solar cells. The world's best level of a surface recombination velocity (SRV) of 1.5 cm/s has been obtained for n-type c-Si wafers passivated with Cat-CVD SiN_x/amorphous-silicon (a-Si) stacked layers.⁷ Cat-CVD can also be used to form a shallow phosphorous (P)-doped layer, called P Cat-doped layer, at a low substrate temperature, such as room temperature.^{8,9} The shallow P doped layer can induce field-effect passivation, which can significantly suppress the recombination of minority carriers at c-Si surface. Although

the shallow doping can be realized by other techniques, such as plasma doping, atomic layer deposition of dopants, and molecular beam epitaxy,¹⁰⁻¹⁴ Cat-doping can significantly avoid damage onto c-Si surface induced by energetic ions since gas molecules are decomposed on a hot wire by catalytic reaction. The advantage makes Cat-doping become a favorable method for the formation of field-effect passivation layers for c-Si. Regarding the application of P Cat-doped layers to passivation technique, it has been already reported that the addition of P Cat-doped layers can reduce the SRV of n-type c-Si passivated with an a-Si film from 5 cm/s to 3 cm/s.¹⁵ In our previous work, we have optimized SiN_x passivation films with refractive index of ~2.0 at wavelength of 630 nm prepared by Cat-CVD for n-type c-Si wafers.¹⁶ The highest effective minority carrier lifetime (τ_{eff}) of 3 ms, corresponding to a low SRV of 5 cm/s, can be obtained for n-type c-Si passivated with Cat-CVD SiN_x films deposited at a low substrate temperature (~100°C) and post annealing. The use of SiN_x films, whose refractive indexes are adjusted to be 2.0 even after decreasing the substrate temperatures, can avoid optical loss due to parasitic absorption in a-Si for SiN_x/a-Si stacked passivation system. The Cat-CVD SiN_x films with high passivation quality and high transparency are suitable for application to c-Si solar cells. As we mentioned above, a P Cat-doped layer can induce field-effect passivation, which is effective in suppressing surface recombination by sending electrons away from the c-Si surface. In this study, in order to obtain even lower SRV on c-Si surface passivated with a SiN_x film, we attempt to apply P Cat-doping for field-effect passivation. The results obtained show that the passivation quality of the SiN_x/P Cat-doped layer/c-Si structure significantly depends on the amount of activated donors in a P Cat-doped layer. Doped substrate temperature and annealing before depositing SiN_x films are important parameters for

^{a)}E-mail: s1240009@jaist.ac.jp. Tel.: +81-761-51-1565, Fax: +81-761-51-1149.

TABLE I. Sample preparation conditions for P Cat-doping and the deposition of SiN_x and a-Si films.

	Doping	a-Si	SiN _x
Gas sources	PH ₃ 20 sccm	SiH ₄ : 10 sccm	SiH ₄ : 8 sccm NH ₃ : 150 sccm
Substrate temperature	80–300 °C	90 °C	100 °C
Pressure	1.0 Pa	0.55 Pa	10 Pa
Catalyzer temperature	1300 °C	1800 °C	1800 °C
Time	30–120 s	30 s	184 s

activating P as donors. The deposition of SiN_x films and post annealing at 350 °C for 30 min are necessary to achieve better interface properties and resulting high τ_{eff} .¹⁶ By the field-effect passivation and defect termination by H atoms, τ_{eff} of as high as 7 ms can be obtained, which corresponds to an SRV of ~ 2 cm/s.

II. EXPERIMENTAL PROCEDURE

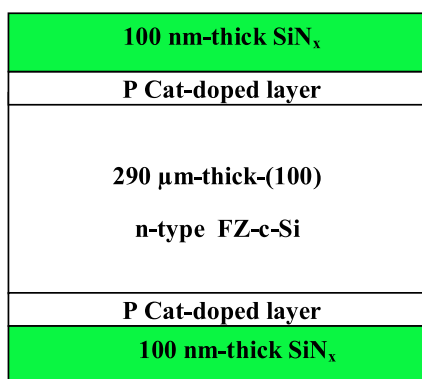
Sample preparation conditions are summarized in Table I. All c-Si wafers were first cleaned in diluted (5%) hydro-fluoric acid (HF) solution for 10 s to remove native oxide. P Cat-doped layers, SiN_x films, and a-Si films were prepared in separate Cat-CVD chambers. A 2.25% helium diluted PH₃ was used as gas source for doping process. In this study, we changed the properties of P Cat-doped layers by changing substrate temperature (T_{s-dope}) and doping time (t_{dope}). The deposition condition of SiN_x films and annealing conditions for the samples after depositing the SiN_x films were same as the optimized conditions, under which high τ_{eff} of 3 ms can be obtained for a SiN_x/c-Si structure.¹⁶ 290- μ m-thick n-type (100) floating-zone (FZ) Si wafers with a resistivity of 2.5 Ω cm and a bulk minority carrier lifetime of >10 ms were used for the investigation of the passivation quality. The structure for τ_{eff} measurement is shown in Fig. 1. In order to investigate the effect of annealing on passivation quality, the P Cat-doped samples were annealed before and after depositing SiN_x films. In this paper, we refer them to “annealing A” and “annealing B,” respectively. Annealing A and annealing B were both conducted in a horizontal tubular furnace in nitrogen atmosphere. We prepared two samples under the same P doping condition at the same batch; one is for a sample with

only annealing B, and the other is for a sample with both annealing A and B. The samples without annealing A were passivated with SiN_x films immediately after P Cat-doping without air break, while the samples with annealing A were taken out from the P doping chamber, followed by furnace annealing and then SiN_x deposition without any additional cleaning prior to deposition. All the SiN_x-deposited samples were finally annealed at 350 °C for 30 min (annealing B). The τ_{eff} was measured by microwave photo-conductivity decay (μ -PCD) (KOBELCO LTA-1510EP) using a 904 nm wavelength pulse laser with a photon density of 5×10^{13} cm⁻², and then was evaluated from the exponential decay of the microwave reflection intensity. The τ_{eff} was measured in position-dependent mapping mode, and τ_{eff} shown below is the maximum value in the 20 \times 20 mm² area mapping. The relationship between τ_{eff} and SRV is described as

$$\frac{1}{\tau_{eff}} = \frac{1}{\tau_{bulk}} + \frac{2SRV}{W}, \quad (1)$$

where τ_{bulk} and W represent minority carrier lifetime in bulk c-Si and wafer thickness, respectively. In this study, we calculated SRV by assuming $\tau_{bulk} = \infty$. We also measured excess-carrier-density-(Δn -) dependent τ_{eff} by quasi-steady-state photoconductance (QSSPC) (WCT-120, Sinton Instruments).

We employed the Hall effect measurement to evaluate the sheet carrier density (N_D) of doped samples and secondary ion mass spectrometry (SIMS) for P concentration. The properties of c-Si wafers used for SIMS measurement are same as those used for τ_{eff} measurement. The SIMS measurement was performed from the back side of the samples after removing most of Si wafers in order to avoid the effect of knock-on and resulting unintentional broadening of P profiles. We used 2900 Ω cm p-type FZ c-Si wafers for the Hall effect measurement. The capture of carriers at defects on c-Si surface and oxidation may affect significantly the results of the Hall effect measurement.^{8,17,18} In order to prevent these effects, a 10-nm-thick a-Si film was deposited on c-Si immediately after P doping without air exposure. In order to know the effect of annealing on N_D , samples were annealed at 350 °C before and after depositing a-Si films. Four Al electrodes were formed by evaporation through a metal hard mask to form the van der Pauw configuration. The samples were annealed at 350 °C for 1 min to make Ohmic contact between Al electrodes and a P Cat-doped layer. Figure 2 shows the cross-sectional schematic of a sample for the Hall effect measurement. The details of the measurement have been described in Ref. 8. The effect of H etching on the

FIG. 1. The cross-sectional schematic of a sample for τ_{eff} measurement.

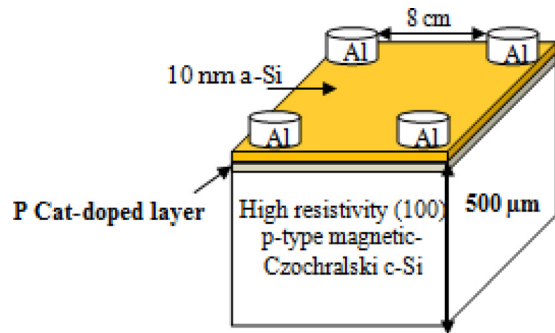


FIG. 2. The cross-sectional schematic of a sample for Hall measurement.

morphology of c-Si surface after P Cat-doping was evaluated by atomic force microscopy (AFM).

III. RESULTS AND DISCUSSION

A. The effect of annealing on P activation as donors and the passivation characteristic of SiN_x/P Cat-doped layer/c-Si structures

Annealing plays an important role in improving the passivation quality of SiN_x/c-Si structures.^{16,19,20} In this study, we first investigate the effect of annealing. c-Si wafers received P Cat-doping at a T_{s-dope} of 80 °C for 1 min, followed by SiN_x film deposition. The samples were then annealed (annealing B) at various annealing temperatures (T_{ab}) for 30 min. Figure 3 shows the dependence of τ_{eff} of a SiN_x/P Cat-doped layer/c-Si structure on T_{ab} . The τ_{eff} of SiN_x/c-Si structures as a function of T_{ab} is also shown for comparison. τ_{eff} starts to increase when T_{ab} exceeds 200 °C for both structures. τ_{eff} reaches the highest value at a T_{ab} of 350 °C, and then decreases with further increase in T_{ab} . The improvement in the τ_{eff} of the SiN_x/c-Si structure is supposed to be due to the effect of defect termination by H atoms during annealing.^{16,19–21} For a SiN_x/P Cat-doped layer/c-Si structure, passivation quality relies not only on H defect

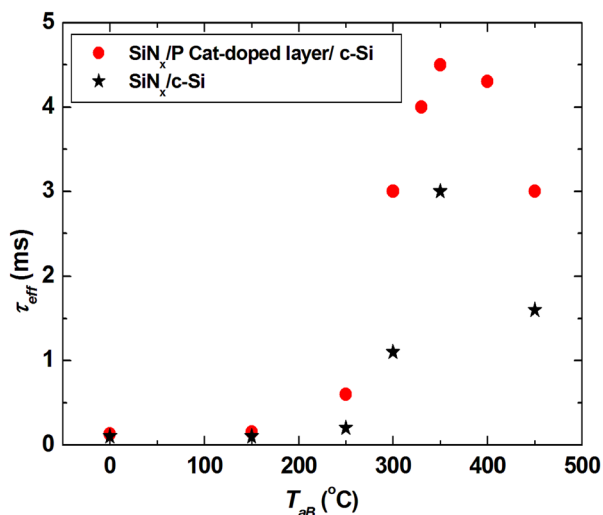


FIG. 3. The dependence of SiN_x/P Cat-doped layer/c-Si structures on T_{ab} at an annealing time of 30 min. τ_{eff} of SiN_x/c-Si structures as a function of T_{ab} is also shown for comparison.

termination but also on field-effect passivation, and increase in T_{ab} might lead to increase in donor (activated P) concentration and resulting enhancement in field-effect passivation. Hayakawa *et al.* have reported that the most inactivated P atoms in a P Cat-doped layer exist in the forms of chemisorbed PH-, PH₂-, and PH₃ (coordinate bond)-type bonds with Si atoms, denoted as PH_x ($x=1-3$).⁸ It has been reported that P and H atoms are major products, while PH- and PH₂- are minor products in the catalytic decomposition of PH₃.²² We thus guess that the extraction of H atoms from PH₃ molecules by formation of H₂ molecules or the addition of H atoms to P atoms on a c-Si surface is possible mechanisms of PH_x production.

PH_x may decompose at high temperature, resulting in the release of P and H atoms. The released H atoms can diffuse to c-Si surface and terminate defects there, and the released P atoms act as donors and contribute to reinforcing field-effect passivation. There have been a number of literatures about the decomposition of P-H bonds using samples with PH₃ adsorbed on c-Si (100).^{23–26} Yu *et al.* have reported that PH₃ molecules are partially dissociated at an annealing temperature of 275 °C for PH₃ adsorbed samples.²³ Tsai *et al.* have reported that PH₃ species are converted to PH₂ species in an adsorbed layer at annealing temperature >317 °C, and a P-H peak disappears when an annealing temperature exceeds 377 °C.²⁵ These facts indicate that PH₂ species are decomposed to P and H atoms at around 300 °C. We can guess that the released H atoms can make bonding with Si atoms and P atoms start to act as donors. In this study, as has been shown in Fig. 3, the τ_{eff} of a SiN_x/P Cat-doped layer/c-Si structure is much higher than that of SiN_x c-Si structure when $T_{ab} \geq 250$ °C. This fact suggests that PH_x starts to decompose efficiently at a T_{ab} of 250 °C. This temperature is quantitatively consistent with the values of the literatures shown above. A T_{ab} of 350 °C is sufficiently high for both PH_x bond breaking in a P Cat-doped layer and defect termination by H in SiN_x films, and higher T_{ab} leads to the desorption of H atoms to atmosphere and resulting in the decrease of τ_{eff} . The highest τ_{eff} can thus be obtained at a T_{ab} of 350 °C for both structures.

On the other hand, contrary to our expectations, the results of the Hall effect measurement show that N_D decreases by annealing. N_D is $1.2 \times 10^{12} \text{ cm}^{-2}$ before annealing, while it reduces to $0.9 \times 10^{12} \text{ cm}^{-2}$ for samples with annealing at 350 °C for 30 min after depositing a-Si films, and to $0.7 \times 10^{12} \text{ cm}^{-2}$ for samples with annealing at the same condition before depositing an a-Si film, a possible reason for reduction in N_D is the diffusion of H atoms from the a-Si film to the P Cat-doped layer, which can cause the formation of more PH_x than PH_x decomposition in a P Cat-doped layer and resulting reduction in N_D . Lower N_D obtained in the sample annealed before depositing an a-Si film may be due to the oxidation of c-Si surface. In order to conduct annealing process, we have to take out the samples to atmosphere. Oxidation can inactivate P at surface c-Si and/or induce the formation of a thin Si oxide film containing P atoms on c-Si surface, which affect the results of the Hall effect measurement. In order to clarify this effect, the samples for the Hall effect measurement

after P Cat-doping at 350 °C were put in air for 15 min before depositing a-Si films. By the additional air exposure, N_D drops from 3×10^{12} to $0.5 \times 10^{12} \text{ cm}^{-2}$, which is a clear evidence of oxidation-induced reduction in N_D . We actually confirmed the formation of a SiO_x film with a thickness of 1.1 nm and a refractive index of 1.5 at a wavelength of 630 nm on c-Si surface by using spectroscopic ellipsometry.

However, the oxidation of c-Si surface does not deteriorate the passivation quality of SiN_x/P Cat-doped layers on c-Si structure. The P Cat-doped layer/c-Si structures with or without annealing A (at 350 °C for 30 min) were put in air for one week. The sample was then passivated with a SiN_x film, and annealed at 350 °C for 30 min (annealing B). For the sample without annealing A, τ_{eff} obtained of 4.4 ms does not differ from τ_{eff} of sample without air exposure. For the sample annealed with annealing B, τ_{eff} obtained is 6.4 ms. The addition of annealing A rather improves the passivation quality of a SiN_x/P Cat-doped layer structure by oxidation. We also investigated the effect of oxidation on τ_{eff} of SiN_x -passivated c-Si samples. Some c-Si wafers received annealing A at 350 °C for 30 min in N_2 atmosphere. The τ_{eff} of $\text{SiN}_x/\text{c-Si}$ structures increases from 50 to 100 μs for samples without annealing B and from 3 to 3.5 ms for samples with annealing B. This indicates that the thermal oxidation of c-Si surface slightly improves the passivation quality of SiN_x films on c-Si wafers. This improvement may be due to reduction in interface state by the formation of a SiO_x film.^{27–29} Furthermore, τ_{eff} of 250 μs is obtained for SiN_x/P Cat-doped layer/c-Si structure with only annealing A. This value is higher than that of a $\text{SiN}_x/\text{c-Si}$ structure annealed with only annealing A. This result indicates that despite reduction in N_D by oxidation, improvement in interface quality by oxidation and defect termination by H atoms released from PH_x can contribute to increase in τ_{eff} . After annealing B, besides the effect of defect termination by H atoms diffused from a SiN_x layer, more PH_x in a P Cat-doped layer can be decomposed, leading to higher donor concentration and more effective defect termination by H atoms, which results in higher τ_{eff} .

On the other hand, as mentioned previously, N_D obtained for an a-Si/P Cat-doped layer/c-Si structure is reduced by annealing at 350 °C for 30 min. Cat-CVD SiN_x films also contain high amount of H atoms, which can diffuse from SiN_x films to c-Si surface and terminate defects or recombine with P atoms to form more PH_x during annealing B. Assuming that reduction in N_D for the SiN_x/P Cat-doped layer/c-Si structures is the same as the case of a-Si/P Cat-doped layer/c-Si after annealing B, N_D of a SiN_x/P Cat-doped layer/c-Si structure decreases by 25%. The sample undergoing both annealing A and B has N_D of $\sim 5 \times 10^{11} \text{ cm}^{-2}$, which is due to the effect of oxidation by annealing A and H diffusion during annealing B. This value of N_D might be high enough for field-effect passivation. The fact that the N_D of the sample receiving both annealing A and B is less than that with only annealing B indicates less effective field-effect passivation. However, the benefit of defect termination by H atoms might overcome the deterioration of field effect and lead to better τ_{eff} for the sample with both annealing A and B.

To understand the effect of annealing A on the passivation quality of SiN_x/P Cat-doped layers, c-Si samples Cat-doped at 80 °C for 1 min were annealed (annealing A) at various annealing temperatures (T_{aA}) for 30 min in the tubular furnace. Samples were then moved to the Cat-CVD system to deposit SiN_x films. Finally, samples were annealed at 350 °C for 30 min (annealing B). Figure 4 shows the τ_{eff} of SiN_x/P Cat-doped layer/c-Si structures after annealing A and B as functions of T_{aA} and annealing time (t_{aA}) for annealing A. N_D as a function of T_{aA} is also shown. One can clearly see that τ_{eff} increases with T_{aA} for samples both with and without process B. τ_{eff} increases when T_{aA} increases and decreases for $T_{aA} \geq 400$ °C. This is probably due to increase in N_D at higher T_{aA} . The increase in N_D is probably due to the decomposition of PH_x at higher T_{aA} and resulting activation of higher amount of P atoms. Additionally, the thermal oxidation of c-Si surface for the samples annealed at high temperature and defect termination by H atoms by annealing might contribute to the formation of a high-quality $\text{SiN}_x/\text{SiO}_x/\text{P}$ Cat-layer and c-Si interface, resulting improvement in τ_{eff} . Because the P Cat-doped layer is very shallow, too high T_{aA} might lead to the desorption of H and P atoms to environment, which can result in decrease in τ_{eff} due to less effective defect termination and field-effect passivation. The complete

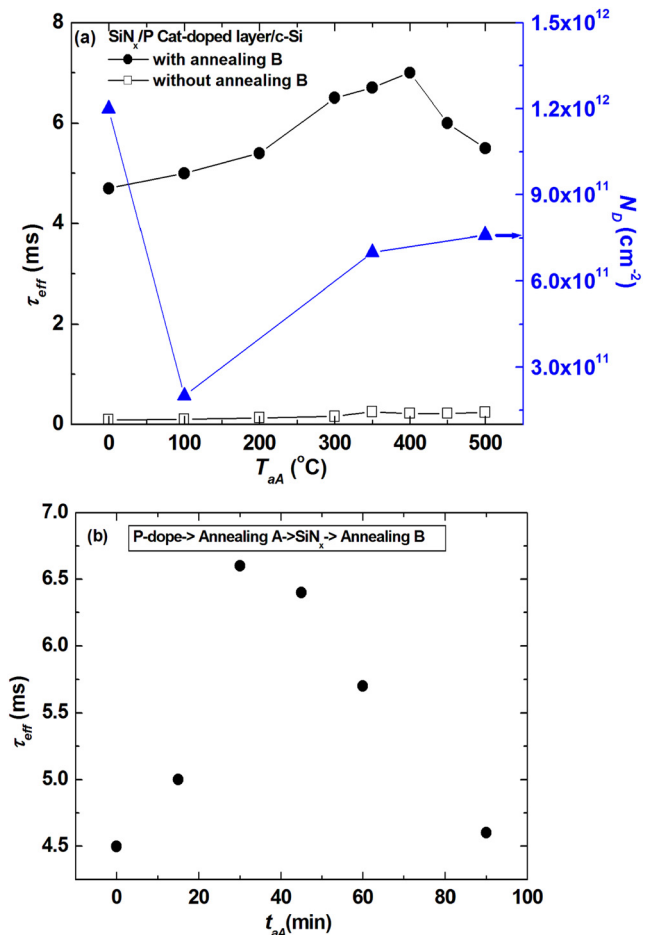


FIG. 4. τ_{eff} of SiN_x/P Cat-doped layer/c-Si structures after annealing A at various T_{aA} for 30 min and t_{aA} at a T_{aA} of 350 °C. Annealing B was conducted at 350 °C for 30 min.

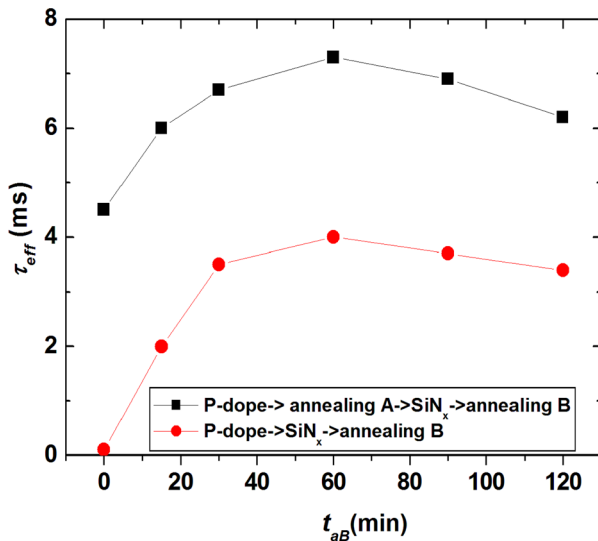


FIG. 5. τ_{eff} of SiN_x/P Cat-doped layer/c-Si structures with and without annealing A as a functions of t_{ab} at a T_{ab} of 350°C. Annealing A was conducted at 400°C for 30 min.

thermal desorption of P atoms from PH_3 adsorbed c-Si surface at high temperature above 550°C was also reported in Ref. 24, in which the desorption of H atoms at 400°C was also observed. The same tendency is seen in the annealing time dependence for annealing A, as shown in Fig. 4(b). T_{aA} of 400°C and t_{aA} of 30 min are thus optimum conditions for annealing A needed to activate P in P Cat-doped layer without H and P desorption, and the highest τ_{eff} obtained for SiN_x/P Cat-doped layer/c-Si structures under the conditions. Figure 5 shows τ_{eff} as a function of the duration of annealing B (t_{ab}). We can see that τ_{eff} is still high for long t_{ab} . The tendencies of the variation of τ_{eff} for both samples are the same. Annealing for 30 min is enough to obtain high passivation quality for the samples. Further increase in t_{ab} does not enhance more the activation of P atoms as well as defect termination. The instability of τ_{eff} due to increase in T_{ab} and t_{ab} may raise a doubt of reduction in τ_{eff} after long time

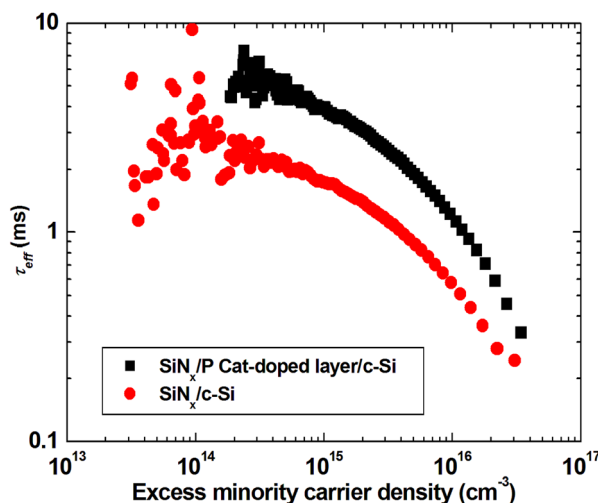


FIG. 6. τ_{eff} as a function of excess carrier density in a SiN_x/P Cat-doped layer/c-Si structure and a $\text{SiN}_x/\text{c-Si}$ structure.

exposure to air even at room temperature. We have confirmed that τ_{eff} of both $\text{SiN}_x/\text{c-Si}$ and SiN_x/P Cat-doped layer/c-Si structures remain original values even after putting in air at room temperature for about 10 months.

In summary, a remarkably high τ_{eff} of ~ 7 ms, which corresponds to an SRV of ~ 2 cm/s, can be achieved for SiN_x/P Cat-doped layer/c-Si samples after annealing A and B. Compared with a $\text{SiN}_x/\text{c-Si}$ structure, the insertion of P Cat-doped layer can reduce an SRV from 5 cm/s to 2 cm/s. The SRV of 4 cm/s has also been achieved when nearly stoichiometric SiN_x films were deposited by plasma-enhanced CVD (PECVD) on 150- μm -thick 3–5 Ω cm n-type Czochralski (Cz) Si wafers after annealed in an industrial firing process.³⁰ An SRV of lower than 10 cm/s has been reported for 1.5 Ω cm p-type Si wafers passivated with stoichiometric SiN_x films.³¹ In these reports, they calculate SRV through τ_{eff} obtained by a contactless photoconductance tester allowing both transient PCD and QSSPC measurements at an Δn of $1 \times 10^{15} \text{cm}^{-3}$. Figure 6 shows τ_{eff} of a SiN_x/P Cat-doped layer/c-Si structure and a $\text{SiN}_x/\text{c-Si}$ structure measured by QSSPC in transient mode. We observed τ_{eff} of ~ 7 ms for SiN_x/P Cat-doped layer/c-Si structure and ~ 3 ms for $\text{SiN}_x/\text{c-Si}$ structure at a Δn of $2.4 \times 10^{14} \text{cm}^{-3}$. At a Δn of $1 \times 10^{15} \text{cm}^{-3}$, τ_{eff} is ~ 4 and 1.8 ms for SiN_x/P Cat-doped layer/c-Si and $\text{SiN}_x/\text{c-Si}$ structures, corresponding to SRVs of 3.6 and 8 cm/s, respectively. Our SRV obtained in this study is the lowest level for n-type c-Si passivated with SiN_x films without firing process or with only low temperature process, which is acceptable for fabrication of a-Si/c-Si hetero-junction solar cells. The remarkable value of our SRV obtained for SiN_x/P Cat-doped layer/c-Si structure highlights the promising application of Cat-CVD technique in high-efficiency n-type c-Si based solar cell fabrication.

B. Effect of T_{s-dope} and doping duration on the passivation characteristic of SiN_x/P Cat-doped layer/c-Si structure

High T_{s-dope} can activate P atoms as donors in a P Cat-doped layer.^{8,9} This can contribute to improvement in field-

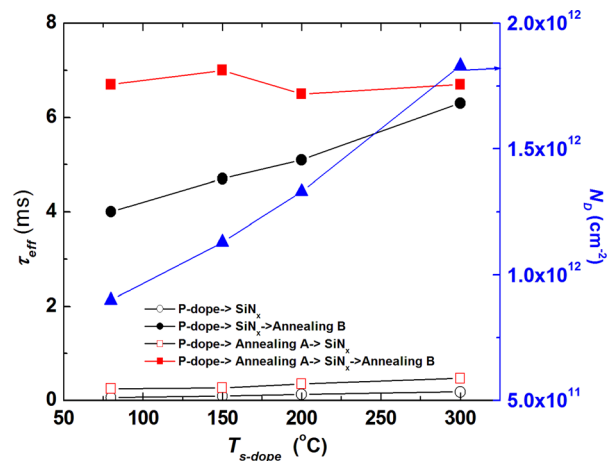


FIG. 7. τ_{eff} of SiN_x/P Cat-doped layer/c-Si samples as a function of T_{s-dope} . N_D as a function of T_{s-dope} before annealing A is also shown. Annealing A was conducted at 400°C for 30 min and annealing B was conducted at 400°C for 30 min.

effect passivation. In this investigation, we prepared P Cat-doped samples at various T_{s-dope} for 1 min. Figure 7 shows τ_{eff} of SiN_x/P Cat-doped layer/c-Si samples as a function of T_{s-dope} with and without annealing A. N_D as a function of T_{s-dope} before annealing is also shown. N_D increases with increase in T_{s-dope} . This may suggest that H atoms desorb from c-Si surface during P Cat-doping at high T_{s-dope} due to the extraction of adsorbed H atoms on c-Si surface by atomic H and/or PH₃.^{8,32,33} As we mentioned above, Umemoto *et al.* have reported that major products in the catalytic decomposition of PH₃ molecules on a heated tungsten catalyzer are P and H atoms.²² Here, we suppose that the reaction of atomic H with adsorbed H and/or PH_x on a c-Si surface and/or PH_x bond breaking are possible mechanisms for H release at high T_{s-dope} . This process might assist P activation. We can see lower H concentration in a sample doped at a T_{s-dope} of 300 °C in a SIMS profile, as shown in Fig. 8 later. The increase in N_D makes small increase in τ_{eff} before annealing. It contributes significantly to improvement in τ_{eff} for the sample doped at high T_{s-dope} when the samples were annealed with annealing B. The samples doped at a T_{s-dope} of 300 °C, which shows N_D of $\sim 2 \times 10^{12} \text{cm}^{-2}$, can reach the highest τ_{eff} of ~ 6 ms.

Figure 7 also shows τ_{eff} of SiN_x/P Cat-doped layer/c-Si samples with annealing A and B as a function of T_{s-dope} . One can see that τ_{eff} does not depend on T_{s-dope} , and all the

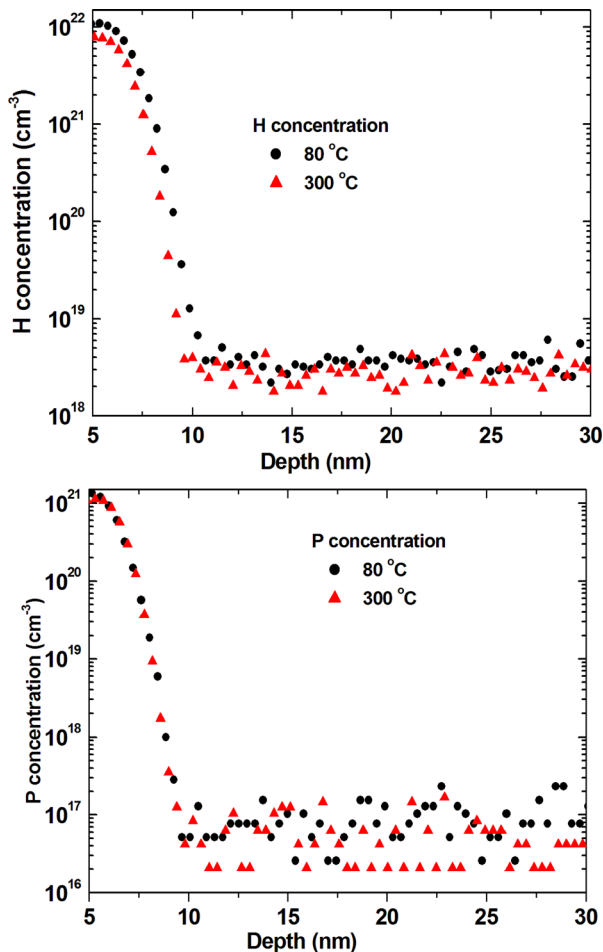


FIG. 8. SIMS profiles of P and H atoms in the samples doped at 80 °C and 300 °C without annealing.

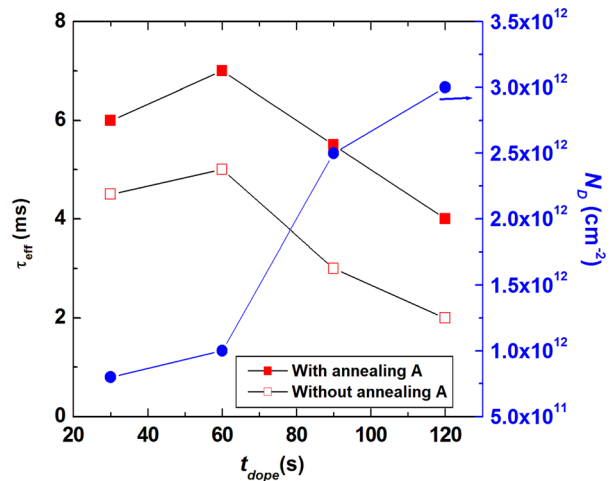


FIG. 9. τ_{eff} of SiN_x/P Cat-doped layer/c-Si samples as a function of t_{dope} with and without annealing A. N_D before annealing is also shown. Annealing A was conducted at 400 °C for 30 min and annealing B was conducted at 400 °C for 30 min.

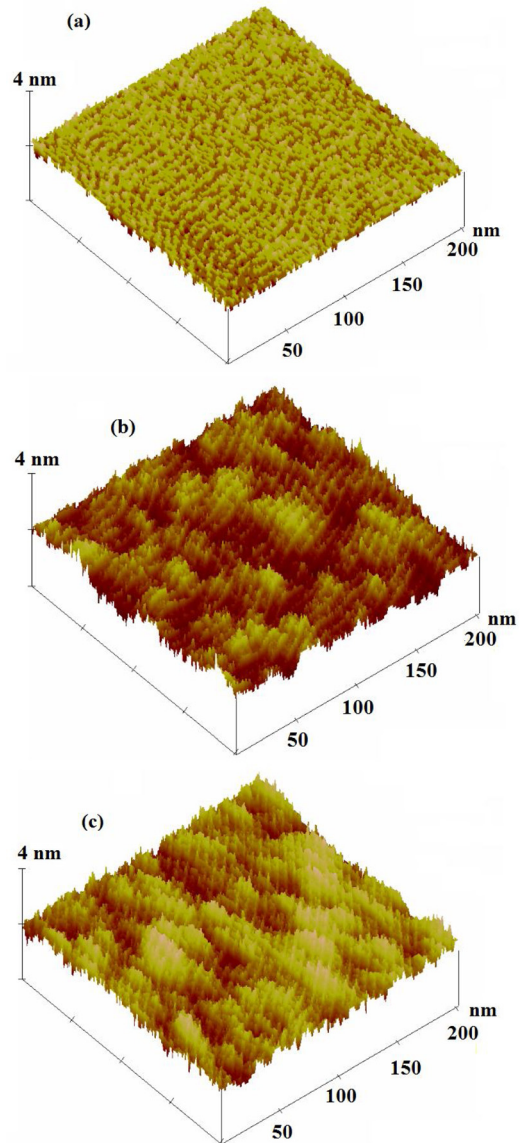


FIG. 10. Surface AFM images of (a) bare c-Si and c-Si Cat-doped for (b) 60 s and (c) 90 s.

samples have constant and high τ_{eff} of 7 ms. This result suggests that P donor concentration is constant in all the samples with annealing before and after SiN_x deposition. Figure 8 shows the SIMS profiles of samples with P Cat-doping at T_{s-dope} of 80 and 300 °C before annealing. We can see no significant difference in the two profiles, suggesting that the activation ratio of P atoms in the two samples is similar.

N_D of a P Cat-doped layer also increases with t_{dope} .⁹ We should therefore concern the effect of doping time on τ_{eff} of SiN_x/P Cat-doped layer/c-Si samples. The samples were doped at 80 °C for 30, 60, 90, and 120 s. The effect of annealing before depositing SiN_x films was also investigated for these samples. Figure 9 shows the τ_{eff} of SiN_x/P Cat-doped layer/c-Si samples as a function of t_{dope} with and without annealing A. N_D without annealing is also shown. Although N_D increases with increase in t_{dope} , τ_{eff} decreases when $t_{dope} \geq 60$ s. For the sample doped for 30 s, τ_{eff} is low due to low N_D . A possible reason for the low τ_{eff} observed in the samples with $t_{dope} \geq 60$ s is the effect of surface etching by radical species during Cat-doping process. Figure 10 shows the surface AFM images of bare c-Si and c-Si doped for 60 s and 90 s. The surface of bare c-Si has a root-mean-square roughness (R_{rms}) of ~ 0.09 nm with the average height of 0.3 nm. As shown in Figs. 10(b) and 10(c), the two P Cat-doped samples have more roughened surfaces, and the surface receiving longer Cat-doping is more seriously etched. The sample with a t_{dope} of 90 s has a R_{rms} of 0.24 nm and average height is 0.9 nm, while they are 0.21 nm and 0.7 nm, respectively, for the sample doped at 60 s. Excess t_{dope} thus rather deteriorates the interface quality, and an optimum t_{dope} exists to obtain high τ_{eff} for SiN_x/P Cat-doped layer/c-Si structure.

IV. CONCLUSION

In conclusion, an extremely low SRV of 2 cm/s can be obtained for the SiN_x/P Cat-doped layer/n-c-Si structure. Annealing plays important roles for improving the passivation quality of SiN_x films and enhancing field-effect passivation. Additional annealing, before depositing SiN_x films (annealing A), enhances the activation of P dopants in a P Cat-doped layer and improves τ_{eff} . Increase in T_{s-dope} increases sheet carrier density, resulting in the improvement of τ_{eff} . τ_{eff} of SiN_x/P Cat-doped/c-Si sample decreases with excessive t_{dope} due to etching effect by radical species during P Cat-doping. An SRV of 2 cm/s is obtained under optimum Cat-doping and annealing conditions for SiN_x films on n-type c-Si wafers, indicating the potential application of Cat-CVD in producing high-efficiency c-Si solar cells. We emphasize that the use of a high transparent SiN_x passivation layer with a P Cat-doped layer can enhance the performance of n-type c-Si solar cells, particularly of back-contact solar cells.

ACKNOWLEDGMENTS

This work was supported by the CREST research program of Japan Science and Technology Agency (JST).

- ¹A. U. Rehman and S. H. Lee, *Sci. World J.* **2013**, 470347.
- ²See <http://www.itrpv.net/> for "International Technology Roadmap for Photovoltaic (ITRPV), SEMI PV Group Europe," 2013.
- ³See http://news.panasonic.net/stories/2014/0416_26881.html for more details about the structure and other properties of 25.6 %-efficiency Panasonic HIT (R) solar cell.
- ⁴D. Macdonald, in The 50th Annual AuSES Conference (Solar 2012), Melbourne, Australia, 6–7 December 2012.
- ⁵A. Goetzberger, J. Knobloch, and B. Vob, *Crystalline Silicon Solar Cells* (John Wiley & Sons, 1998), Vol. 87.
- ⁶H. Matsumura, *J. Appl. Phys.* **65**, 4396 (1989).
- ⁷K. Koyama, K. Ohdaira, and H. Matsumura, *Appl. Phys. Lett.* **97**, 082108 (2010).
- ⁸T. Hayakawa, Y. Nakashima, K. Koyama, K. Ohdaira, and H. Matsumura, *Jpn. J. Appl. Phys. Part 1* **51**, 061301 (2012).
- ⁹T. Hayakawa, T. Ohta, Y. Nakashima, K. Koyama, K. Ohdaira, and H. Matsumura, *Jpn. J. Appl. Phys. Part 1* **51**, 101301 (2012).
- ¹⁰H. J. Gossmann and F. C. Unterwald, *Phys. Rev. B* **47**, 12618 (1993).
- ¹¹F. J. Ruess, L. Oberbeck, M. Y. Simmons, K. E. J. Goh, A. R. Hamilton, T. Hallam, S. R. Schofield, N. J. Curson, and R. G. Clark, *Nano Lett.* **4**, 1969 (2004).
- ¹²Y. Shimamune, M. Sakuraba, J. Murota, and B. Tillack, *Appl. Surf. Sci.* **224**, 202 (2004).
- ¹³N. L. Matthey, M. G. Dowsett, E. H. C. Parker, T. E. Whall, S. Taylor, and J. F. Zhang, *Appl. Phys. Lett.* **57**, 1648 (1990).
- ¹⁴H. P. Zeindl, T. Wegehaupt, I. Eisele, H. Oppolzer, H. Reisinger, G. Tempel, and F. Koch, *Appl. Phys. Lett.* **50**, 1164 (1987).
- ¹⁵H. Matsumura, M. Miyamoto, K. Koyama, and K. Ohdaira, *Sol. Energy Mater. Sol. Cells* **95**, 797 (2011).
- ¹⁶T. C. Thi, K. Koyama, K. Ohdaira, and H. Matsumura, *Jpn. J. Appl. Phys. Part 1* **53**, 022301 (2014).
- ¹⁷W. Clarke, X. Zhou, A. Fuhrer, T. Reusch, and M. Simmons, *Physica E* **40**, 1566 (2008).
- ¹⁸H. Luth, *Solid Surfaces, Interfaces and Thin Films* (Springer, Heidelberg, 2010), p. 323.
- ¹⁹V. Yelundur, A. Rohatgi, J. I. Hanoka, and R. Reedy, in *Proceedings of the 19th European Photovoltaic Solar Energy Conference, Paris, France, June 2004* (ETA-Florence, 2004), pp. 951–954.
- ²⁰B. Sopori, Y. Zhang, R. Reedy, K. Jones, Y. Yan, M. A. Jassim, B. Bathey, and J. Kalejs, in *Proceedings of the 31st Photovoltaic Specialists Conference, Orlando, FL, January 2005* (IEEE, 2005), pp. 1039–1042.
- ²¹J. Hong, W. M. M. Kessels, W. J. Soppe, A. W. Weeber, W. M. Arnolbik, and M. C. M. van de Sande, *J. Vac. Sci. Technol., B* **21**, 2123 (2003).
- ²²H. Umemoto, Y. Nishihara, T. Ishikawa, and S. Yamamoto, *Jpn. J. Appl. Phys. Part 1* **51**, 086501 (2012).
- ²³M. L. Yu, J. J. Vitkavage, and B. S. Meyerson, *J. Appl. Phys.* **59**, 4032 (1986).
- ²⁴M. L. Yu and B. S. Meyerson, *J. Vac. Sci. Technol., A* **2**, 446 (1984).
- ²⁵H. W. Tsai and D. S. Lin, *Surf. Sci.* **482–485**, 654 (2001).
- ²⁶S. R. Schofield, N. J. Curson, O. Warschkow, N. A. Marks, H. F. Wilson, M. Y. Simmons, P. V. Smith, M. W. Radny, D. R. McKenzie, and R. G. Clark, *J. Phys. Chem. B* **110**, 3173 (2006).
- ²⁷H. Nagayoshi, M. Ikeda, M. Yamaguchi, T. Uematsu, T. Saitoh, and K. Kamisako, *Jpn. J. Appl. Phys. Part 1* **36**, 5688 (1997).
- ²⁸Y. Lee, W. Oh, V. A. Dao, S. W. Hussain, and J. Yi, *Int. J. Photoenergy* **2012**, 753456.
- ²⁹S. W. Glunz, *Adv. Optoelectron.* **2007**, 97370.
- ³⁰S. Duttgupta, B. Hoex, and A. G. Aberle, in the 22nd International Photovoltaic Science and Engineering Conference, Hangzhou, China, November 2012.
- ³¹J. Schmidt and M. Kerr, *Sol. Energy Mater. Sol. Cells* **65**, 585 (2001).
- ³²F. Khanom, A. Aoki, F. Rahman, and A. Namiki, *Surf. Sci.* **536**, 191 (2003).
- ³³Y. Narita, Y. Kihara, S. Inanaga, and A. Namiki, *Surf. Sci.* **603**, 1168 (2009).